C-KIT mutation cooperates with full-length AML1-ETO to induce acute myeloid leukemia in mice

Yue-Ying Wang[a,1], Li-Juan Zhao[a,b,1], Chuan-Feng Wu[a,b], Ping Liu[a], Lin Shi[a], Yang Liang[a], Shu-Min Xiong[a], Jian-Qing Mi[a], Zhu Chen[a,2], Ruibao Ren[c,2], and Sai-Juan Chen[a,2]

[a]State Key Laboratory of Medical Genomics and Shanghai Institute of Hematology, Rui Jin Hospital Affiliated to Shanghai Jiao Tong University (SJTU) School of Medicine, Shanghai 200025, China; [b]Institute of Health Sciences, Shanghai Institutes for Biological Sciences and Graduate School, Chinese Academy of Sciences and SJTU School of Medicine, Shanghai 200025, China; and [c]Rosenstiel Basic Medical Sciences Research Center and Department of Biology, Brandeis University, Waltham, MA 02454

Contributed by Zhu Chen, December 30, 2010 (sent for review November 27, 2010)

The full-length *AML1-ETO* (*AE*) fusion gene resulting from t(8;21)(q22;q22) in human acute myeloid leukemia (AML) is not sufficient to induce leukemia in animals, suggesting that additional mutations are required for leukemogenesis. We and others have identified activating mutations of *C-KIT* in nearly half of patients with t(8;21) AML. To test the hypothesis that activating *C-KIT* mutations cooperate with *AE* to cause overt AML, we generated a murine transduction and transplantation model with both mutated *C-KIT* and *AE*. To overcome the intracellular transport block of human C-KIT in murine cells, we engineered hybrid C-KIT (HyC-KIT) by fusing the extracellular and transmembrane domains of the murine c-Kit in-frame to the intracellular signaling domain of human C-KIT. We showed that tyrosine kinase domain mutants HyC-KIT N822K and D816V, as well as juxtamembrane mutants HyC-KIT 571+14 and 557-558Del, could transform murine 32D cells to cytokine-independent growth. The protein tyrosine kinase inhibitor dasatinib inhibited the proliferation of 32D cells expressing these C-KIT mutants, with potency in the low nanomolar range. In mice, HyC-KIT N822K induced a myeloproliferative disease, whereas HyC-KIT 571+14 induces both myeloproliferative disease and lymphocytic leukemia. Interestingly, coexpression of AE and HyC-KIT N822K led to fatal AML. Our data have further enriched the two-hit model that abnormalities of both transcription factor and membrane/cytosolic signaling molecule are required in AML pathogenesis. Furthermore, dasatinib prolonged lifespan of mice bearing AE and HyC-KIT N822K-coexpressing leukemic cells and exerted synergic effects while combined with cytarabine, thus providing a potential therapeutic for t(8;21) leukemia.

stem cell factor | mouse model | targeted therapy | combinatorial therapy | interleukin-3

The t(8;21)(q22;q22) translocation, which generates *AML1-ETO* (*AE*) fusion gene, is one of the most common chromosomal abnormalities detected in acute myeloid leukemia (AML) (1, 2). A high-level expression of full-length *AE* can be detected in all patients with t(8;21) and is thus considered to play a fundamental role in this type of leukemia. Studies of several murine models have demonstrated, nevertheless, that *AE* alone is not sufficient to induce AML, in that no leukemia development was found in mice carrying an *AE* knockin allele (3, 4) in *AE*-transgenic mice (5, 6) or in wild-type (WT) mice that received a transplant of bone marrow (BM) cells transduced retrovirally with *AE* (7). Of note, in the presence of additional mutations [e.g., mutagen *N*-ethyl-*N*-nitrosourea (6), mutations of *FLT3* (8), or the *TEL-PDGFR*β fusion gene (9)], *AE* induces an AML phenotype. Moreover, ectopically expression of *AE9a* (a C-terminally truncated variant of *AE*) can induce AML in mice (10). These results indicate that full-length *AE* may need cooperation with other molecular events in initiating AML.

Genetic abnormalities affecting transcription factors and mutations affecting genes involved in signal transduction represent two classes of the most frequently detected genetic events in human leukemia (11, 12). A number of experiments in mice have favored a model of pathogenesis of acute leukemia in which the two groups of genetic alterations are both required in causing full-blown acute leukemia (13, 14). Indeed, studies in patients have demonstrated that activating mutations involving signal transduction pathways (*C-KIT*, *FLT3*, *NRAS*) are common in *AE*-positive AML (15, 16), and the frequency of *C-KIT* mutations in this type of leukemia can be as high as 48% (17, 18). However, the potential cooperation between *C-KIT* mutants and full-length *AE* has not yet been tested, although a recent report suggested that murine *c-KitD814H* could moderately accelerate the leukemogenic process of *AE9a* (19).

In this study, we addressed the leukemogenic potential of *C-KIT* mutations and *AE* with a murine BM transduction and transplantation model. We found that mice with BM cells coexpressing AE and HyC-KIT N822K, a common C-KIT mutation found in t(8;21)(q22;q22) AML, developed AML. Malignant blasts from these mice were easily transplanted into secondary recipients. Our results also suggested beneficial effects of using tyrosine kinase inhibitors in the treatment of leukemia with activated C-KIT mutations.

Results

Transforming Potentials of C-KIT Mutations in Vitro. Although the intracellular signaling domains of the human C-KIT and murine c-Kit proteins share 93% homology, the extracellular domains of human C-KIT and mouse c-Kit are only 74% homologous and are not structurally identical (20). It has been reported that the human C-KIT D816V had no transforming ability and failed to induce disease in mice, owing to an intracellular transportation block, whereas hybrid C-KIT D816V that was generated by fusing the extracellular and transmembrane domains of the murine c-Kit in-frame to the intracellular signaling domain of human C-KIT induced fatal myeloproliferative disease (MPD) in mice (21). The N822K mutation occurring in activating loop of C-KIT is one of the most common gain-of-function mutations associated with AML (17). To test transforming activities in vitro and in vivo of C-KIT N822K and other mutants, we generated retroviral constructs containing hybrid C-KIT mutations (HyC-KIT N822K and other HyC-KITs) with the murine *c-Kit* encoding extracellular and transmembrane domains fused in-frame to the intracellular domain of human *C-KIT* sequences (Fig. 1 *A* and *C*). Their expression in infected NIH 3T3 cells was validated by Western blotting (Fig. 1*B*). We also checked the surface expression of HyC-KIT proteins using flow cytometry. The WT hybrid C-KIT receptor and HyC-KIT N822K were expressed at high levels on the cell surface of murine NIH 3T3 cells (Fig. 1*D*), whereas hu-

Author contributions: Z.C. and S.-J.C. designed research; Y.-Y.W., L.-J.Z., C.-F.W., P.L., L.S., and Y.L. performed research; S.-M.X., J.-Q.M., Z.C., R.R., and S.-J.C. analyzed data; and Y.-Y.W., Z.C., R.R., and S.-J.C. wrote the paper.

The authors declare no conflict of interest.

[1]Y.-Y.W. and L.-J.Z. contributed equally to this work.

[2]To whom correspondence may be addressed. E-mail: zchen@stn.sh.cn, ren@brandeis.edu, or sjchen@stn.sh.cn.

This article contains supporting information online at www.pnas.org/lookup/suppl/doi:10.1073/pnas.1019625108/-/DCSupplemental.

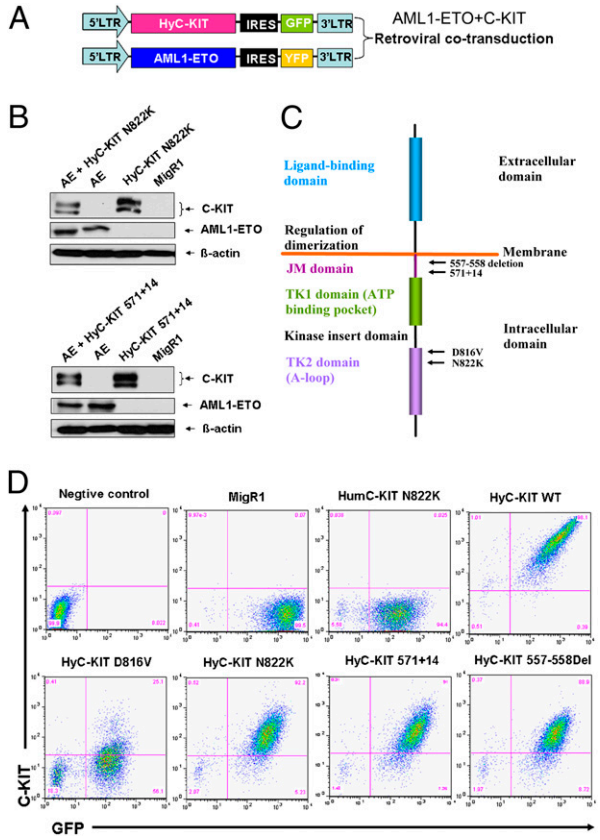

Fig. 1. Schematic diagram of retroviral constructs and analysis of C-KIT and AML1-ETO expression. (*A*) MSCV-based retroviral constructs used to express AML1-ETO and HyC-KIT with fluorescent markers GFP and YFP. (*B*) Whole-cell protein lysates from retroviral-infected NIH 3T3 cells were analyzed by immunoblotting with anti–c-Kit antibody recognizing intracellular domain of both human C-KIT and murine c-Kit proteins, anti-AML1, or anti–β-actin antibodies. (*C*) Schematic representation of C-KIT showing location of functional domains and specific C-KIT mutations used in our study. (*D*) Flow cytometry analysis of the expression of HumC-KIT N822K, WT hybrid C-KIT receptor, mutant HyC-KIT N822K, HyC-KIT D816V, HyC-KIT 571+14, and HyC-KIT 557-558Del on the cell surface of the retroviral-infected NIH 3T3 cells.

man C-KIT (HumC-KIT) N822K was not detectable. The HyC-KIT D816V was detected on the cell surface, albeit at a reduced level compared with that of HyC-KIT N822K.

The biological consequences of expressing HyC-KIT mutants in 32D cells were analyzed by comparing the proliferative response of 32D cells with the control GFP (MigR1), WT HyC-KIT, and HumC-KIT N822K under different growth conditions. The surface expression of HyC-KIT receptors was detected in 32D cells, with a similar pattern as in NIH 3T3 cells. Proliferation assays showed that both HyC-KIT N822K and HyC-KIT D816V could rapidly transform 32D cells to cytokine independence, whereas 32D cells expressing the control GFP and WT HyC-KIT were strictly dependent on IL-3 for their growth (Fig. 2*A*). As expected, HumC-KIT N822K was unable to transform 32D cells.

Activating mutations involving the C-KIT juxtamembrane domain occur in some cases of mast cell disease (22), AML (15, 16), and two thirds of gastrointestinal stromal tumors (GISTs) (23, 24). Although C-KIT 557-558Del mutation is most common in GISTs as reported (24), the internal tandem duplication-type C-KIT 571+14 mutation occurring in juxtamembrane domain was found in our previous studies of t(8;21) AML (17). We compared the ability of these two C-KIT mutants to transform murine cells and found that both HyC-KIT 571+14 and HyC-KIT 557-558Del caused overgrowth of murine 32D cells in the absence of IL-3, even more rapidly than HyC-KIT N822K and

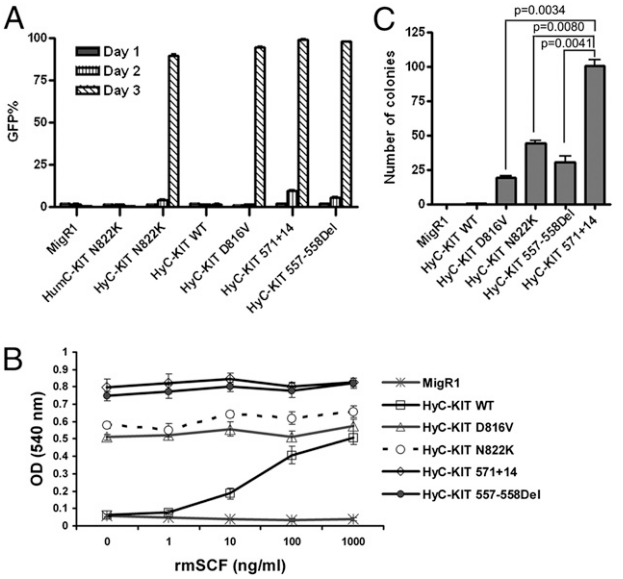

Fig. 2. Activating mutations of C-KIT receptor tyrosine kinase caused transformation of murine 32D cells to cytokine-independent growth. (*A*) 32D cells expressing different *C-KIT* alleles were starved of IL-3, and viable GFP positive cells were measured by FACS. Cells expressing HyC-KIT N822K, HyC-KIT D816V, HyC-KIT 571+14, and HyC-KIT 557-558Del grew rapidly after IL-3 withdrawal. Mock-infected, vector-alone, HumC-KIT N822K, and HyC-KIT WT control cell populations did not grow in the absence of IL-3. (*B*) Proliferation of 32D cells expressing *C-KIT* alleles in response to various concentrations of rmSCF. Transduced 32D cells were washed three times to remove IL-3 and restimulated with rmSCF with various dosages. Cell proliferation was measured by MTT assay. (*C*) Anchorage-independent growth of NIH 3T3 cells expressing mutant C-KIT receptors. Sorted GFP$^+$ cells were seeded in soft-agar, and colonies were counted at day 14. Statistical analysis of the number of colonies shows HyC-KIT 571+14 has a significantly higher transforming potential than other C-KIT mutants ($P < 0.01$).

HyC-KIT D816V (Fig. 2*A*). The surface expression of HyC-KIT 571+14 and HyC-KIT 557-558Del were detected in both NIH 3T3 cells and 32D cells (Fig. 1*D*).

We also examined the responses of 32D cells expressing HyC-KIT mutants to the c-Kit ligand (stem cell factor, SCF). We found that cells with expression of HyC-KIT WT responded to recombinant mouse SCF (rmSCF) in a dose-dependent manner, whereas those expressing HyC-KIT D816V, HyC-KIT N822K, HyC-KIT 571+14, or HyC-KIT 557-558Del lost responsiveness to SCF (Fig. 2*B*). These results indicate that C-KIT mutations induce ligand-independent activation of the C-KIT receptor.

To further determine the transforming abilities of the C-KIT mutations, we expressed both WT and mutant C-KIT receptors by retroviral infection of NIH 3T3 cells. GFP-positive cells were sorted by FACS and introduced into a soft-agar colony assay. MigR1 and *HyC-KIT WT* were unable to form colonies in the absence of c-Kit ligand. In contrast, NIH 3T3 cells expressing HyC-KIT N822K, HyC-KIT D816V, HyC-KIT 571+14, or HyC-KIT 557-558Del formed numerous colonies in the absence of c-Kit ligand (Fig. 2*C*). HyC-KIT 571+14 displayed a significantly higher transforming potential than other C-KIT mutants ($P < 0.01$) (Fig. 2*C*).

Responses of C-KIT Mutations to Inhibition by Dasatinib and Imatinib. Imatinib is a potent inhibitor of the Abelson murine leukemia viral oncogene homolog (ABL), platelet-derived growth factor receptor (PDGFR), and C-KIT tyrosine kinases and is now the standard frontline therapy for chronic myelogenouse leukemia and advanced GISTs. Although imatinib is a potent inhibitor of the WT C-KIT and the juxtamembrane domain mutations of C-KIT found in most GISTs, C-KIT with activation loop mutations found in AML and

imatinib-resistant GISTs are resistant to imatinib used at clinically therapeutic concentrations (25). This is because imatinib only binds tyrosine kinases with an inactive conformation, but activation loop mutations in C-KIT were believed to activate the kinase and stabilize its active conformation (26–28). Dasatinib, originally identified as a dual sarcoma (SRC)/ABL tyrosine kinase inhibitor, can bind tyrosine kinases in their active conformation and inhibit many BCR/ABL mutants that are resistant to imatinib (29). It was recently shown that dasatinib can inhibit C-KIT with D816 mutations, an activation loop mutation that is resistant to imatinib (30). We tested the activity of dasatinib against KIT juxtamembrane domain mutations and activation loop of tyrosine kinase domian mutations using the 32D cell line that expressed the C-KIT mutants. Dasatinib inhibited cellular proliferation of 32D cells expressing HyC-KIT 557-558Del, HyC-KIT 571+14, HyC-KIT N822K, and HyC-KIT D816V in a dose-dependent manner, with IC_{50} of 0.36 nM, 1.92 nM, 1.12 nM, and 23.65 nM, respectively (Fig. 3 *A–D*). Dasatinib had no effect on control 32D cells with MigR1.

We also compared the sensitivities of cells bearing C-KIT mutations to inhibition by Imatinib. Interestingly, whereas cells with HyC-KIT D816V exhibited resistance to imatinib, those with HyC-KIT N822K were sensitive to the compound, albeit to a lesser extent compared with those expressing the juxtamembrane domain mutants HyC-KIT 557-558Del and HyC-KIT 571+14 (Fig. 3*E*). These data suggest that dasatinib can be a potent inhibitor of both the juxtamembrane and the activation loop mutants of C-KIT associated with AML and GISTs, and that some activation loop mutants including C-KIT N822K can still be sensitive to imatinib.

HyC-KIT N822K Induces MPD in Mice. To characterize the ability of C-KIT mutations to induce disease in vivo, we performed transplantation experiments using mouse BM cells infected with the retroviral vectors expressing C-KIT mutants. Consistent with our data that human C-KIT N822K was unable to transform murine cells in vitro, we found that mice transplanted with HumC-KIT N822K did not show any diseases after 18 mo of observation. In contrast, mice transplanted with HyC-KIT N822K developed MPD, with a median survival of 171.5 d (Fig. 4*A*). HyC-KIT N822K-induced disease was characterized by massive expansion of maturing myeloid cells and infiltration of peripheral blood, BM, spleen, and liver evidenced by hepatosplenomegaly and increased $GFP^+/Mac\text{-}1^+/Gr\text{-}1^+$ cells in peripheral blood, BM, liver, and spleen (Fig. 4*C* and Table 1).

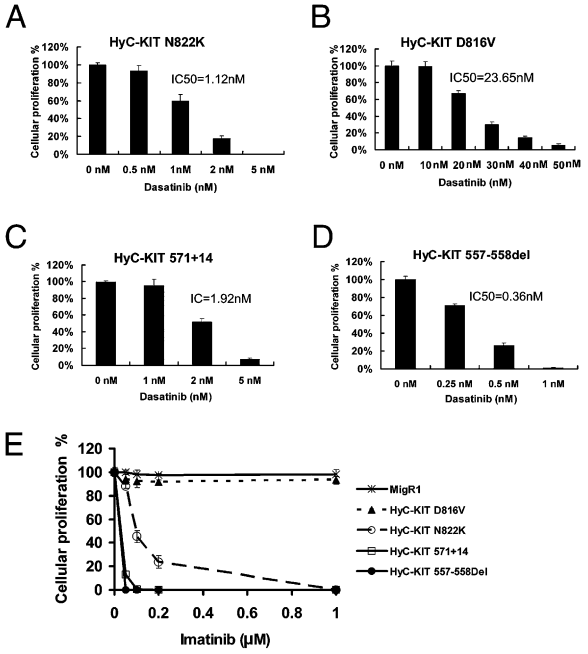

Fig. 3. Response of 32D cells expressing C-KIT mutations to tyrosine kinase inhibitors. Cells were treated with varying concentrations of dasatinib (*A–D*) or imatinib (*E*) for 48 h, and cellular proliferation was measured by counting viable cells.

HyC-KIT 571+14 Induces Both MPD and B-Lymphocytic Leukemia. To investigate the leukemogenic potential of HyC-KIT 571+14, we expressed this mutant protein in primary murine BM cells and monitored transplanted recipient mice for the development of disease. Two thirds of the mice transplanted with HyC-KIT 571+14 died of a rapidly fatal B-lymphocytic leukemia, characterized by increased $GFP^+/B220^+/CD19^+$ cells, leukocytosis, splenomegaly, and central nervous system infiltration (Fig. 4*D* and Table 1). The earliest onset of B-lymphocytic leukemia in these mice occurred at 50 d after transplantation. The other mice expressing HyC-KIT 571+14 developed MPD with overwhelming granulocytosis (Fig. 4*E*).

HyC-KIT N822K Cooperates with AE to Cause a Transplantable AML. To test the functional significance of the association of *AE* with *C-KIT* mutations, we carried out BM transplantation studies using murine BM cells transduced with both AE and C-KIT mutant. We chose to examine the effects of C-KIT N822K on the basis of the clinical evidence that it is the most frequent *C-KIT* mutation coexpressed with *AE* in t(8;21) AML. We hypothesized that AE would cooperate with C-KIT N822K to disrupt myeloid differentiation, resulting in an accumulation of immature myeloid cells characteristic of AML. Murine stem cell virus (MSCV)-based retroviral constructs carrying *HyC-KIT N822K* upstream of an internal ribosomal entry site–green fluorescent protein (IRES-GFP) cassette or *AE* upstream of an IRES–yellow fluorescent protein (IRES-YFP) cassette were generated to cotransduce and track hematopoietic cells expressing HyC-KIT N822K (GFP^+), AE (YFP^+), or both HyC-KIT N822K and AE (GFP^+/YFP^+) in vivo (Fig. 1 *A* and *B*). Transduced cells were then transplanted into lethally irradiated syngeneic recipient mice.

Recipient mice of *AE* alone transduced BM appeared healthy and displayed normal hematopoiesis in the peripheral blood during a 200-d observation period (Fig. 4*A* and Table 1). In contrast, recipients of *AE* and *HyC-KIT N822K* doubly transduced BM died of aggressive acute leukemia after a median latency of 177.5 d after transplantation (Fig. 4*A* and Table 1). Expression of the AE and HyC-KIT N822K was detected in the leukemic mice using RT-PCR and Western blotting analysis (Fig. S1*C*). These mice manifested anemia, high white blood cell (WBC) count, and hepatosplenomegaly (Fig. 4*F* and Table 1). High numbers (35–60%) of blast cells were present in the peripheral blood and BM. Flow cytometric analysis of cells from the peripheral blood, BM, spleen, and liver of leukemic mice showed that the GFP/YFP-coexpressing cells predominantly contain immature blasts ($c\text{-}Kit^+$, $Mac1^-$, $Gr1^-$, $CD19^-$, $B220^-$, $CD3^-$, $TER119^-$, and $F4/80^-$) (Fig. 4*F*).

To further address the cooperation between AE and mutant C-KIT N822K, we performed secondary transplantation by injecting freshly isolated splenocytes from terminally ill mice i.v. into sublethally irradiated (450 cGy) BALB/c female mice (n = 5). Approximately 1.5×10^6 leukemia cells were transplanted into each secondary recipient. All of these mice rapidly developed an AML phenotype similar to that seen in primary mice 20–35 d after transplantation (Fig. 4*A* and Fig. S1). Therefore, in contrast to the phenotypes observed when either oncoprotein was expressed alone, coexpression of AE and HyC-KIT N822K resulted in transplantable fatal AML in mice.

In Vivo Efficacy of Dasatinib on t(8;21) Murine Model. We next used our model system to test whether dasatinib is also effective at treating t(8;21) AML in mice. BALB/c mice were sublethally irradiated and injected i.v. with 1×10^6 leukemic cells coexpressing AE and HyC-KIT N822K. Dasatinib and/or Ara-C treatment was started on day 3, and overall survival was measured from day

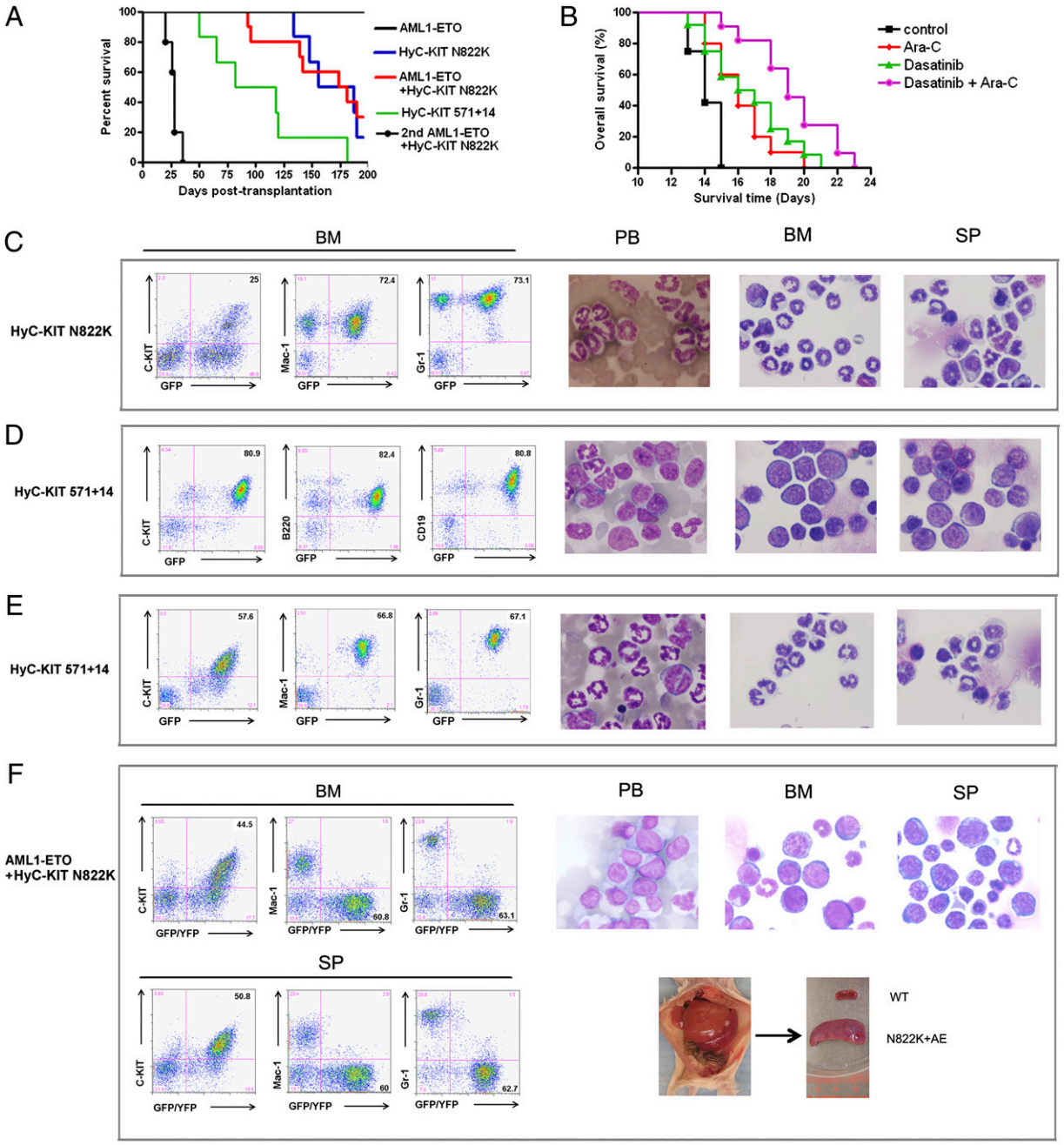

Fig. 4. Mutant HyC-KIT with or without AE induced distinct hematopoietic diseases in mice. (*A*) Kaplan-Meier survival curves of mice transplanted with BM cells transduced with the indicated retroviral construct. Mice transplanted with HyC-KIT N822K-expressing BM cells developed MPD. HyC-KIT 571+14 induced both MPD and acute B-lymphocytic leukemia in mice. Mice transplanted with BM cells coexpressing AML1-ETO and HyC-KIT N822K developed fatal AML. AE + HyC-KIT N822K secondary recipients (n = 5) developed a rapidly fatal myeloid leukemia similar to the primary recipients demonstrating transplantability of the leukemic phenotype. (*B*) Kaplan-Meier survival curves of control and treated mice with AE + HyC-KIT N822K induced AML. Secondary recipient mice were transplanted with splenocytes from a primary leukemic mouse and then treated with vehicle (n = 12), 25 mg/kg Ara-C (n = 12), 10 mg/kg dasatinib (n = 12), or dasatinib plus Ara-C (n = 11). Dasatinib and Ara-C improved overall survival time. A synergic effect was seen when dasatinib was combined with Ara-C. (*C–F*) Immunophenotype analysis (*Left*) and morphological analysis (*Right*) of hematopoietic cells from representative diseased mice. Peripheral blood (PB) smears, BM, and spleen (SP) cytocentrifugation were stained by Wright-Giemsa staining. Gross examination of a representative moribund AE + HyC-KIT N822K mouse shows hepatosplenomegaly (*F*).

0 to the date of death. Treatment with 25 mg/kg Ara-C resulted in strong myelosuppression but was tolerated well. In mice treated with dasatinib and/or Ara-C, the spleen volume was reduced. Moreover, dasatinib and Ara-C significantly delayed disease onset in this model and showed an increase in survival time, extending the median overall survival from 14 to 16.5 d (dasatinib 10 mg/kg, $P <$ 0.01) or 16 d (Ara-C 25 mg/kg, $P < 0.01$), relative to the control group (Fig. 4*B*). Combined use of dasatinib and Ara-C further prolonged survival of mice ($P < 0.05$ compared with Ara-C and dasatinib treatment groups), with median survival of 19 d (Fig. 4*B*).

Discussion

Activating mutations of C-KIT are common in t(8;21) AML (17, 18) and associate with poor prognosis (31, 32). Here we report that

Table 1. Hematopathologic characteristics of analyzed experimental mice

Construct	*n*	Disease	Median survival (d)	WBC* ($\times 10^3/\mu L$)	Hematocrit† (%)	Liver weight (g)	Spleen weight (g)	Paralysis
AE	6	None	Undefined	12.4–23.6	51.8 ± 4.1	1.13 ± 0.15	0.10 ± 0.03	–
HumC-KIT N822K	12	None	Undefined	10.4–24.3	54.0 ± 3.0	1.15 ± 0.22	0.09 ± 0.04	–
HyC-KIT N822K	6	MPD	171.5	111.2–325.3	29.0 ± 5.0	1.78 ± 0.20	0.45 ± 0.18	–
AE+HyC-KIT N822K	10	AML	177.5	182.9–256.6	21.0 ± 5.6	2.11 ± 0.34	0.54 ± 0.19	–
HyC-KIT 571+14	6	B-ALL; MPD	100	26.4–250.3	28.8 ± 13.9	1.43 ± 0.39	0.41 ± 0.21	+

B-ALL, B-acute lymphocytic leukemia.
*WBC count is given as the range of WBCs for the particular group.
†Hematocrit, liver, and spleen weights are average ± SD.

C-KIT N822K, one of the most common C-KIT mutations found in t(8;21) AML, cooperates with the full-length AE in the induction of a transplantable AML in mice. The finding is in support of the idea that C-KIT mutations play a critical role in the pathogenesis of t(8;21) AML. Our data provide further evidence to the model of leukemogenesis in which the collaboration of two classes of genetic alterations, one affecting transcription factors associated with hematopoietic differentiation and the other affecting signal transduction pathways associated with cell proliferation, is necessary for the malignant transformation of hematopoietic stem/progenitor cells. In this regard, a previous report also demonstrated an AE and FLT3-length mutation cooperation in inducing AML or lymphoblastic leukemias of B and T cell type in mice (8), although the rate of FLT3 mutation in t(8;21) AML is much lower compared with C-KIT mutations. The identification of activating receptor tyrosine kinase (RTK) mutations in *AE*-positive leukemia together with experimental evidence that these two classes of genetic alterations collaborate in leukemogenesis will improve the understanding of the pathogenesis of t(8;21) leukemia and provide useful animal models for testing innovative therapeutic approaches in the future.

Our data show that different C-KIT mutations have distinct leukemogenic potentials. The internal tandem duplication-type juxtamembrane domain mutant C-KIT 571+14 has the highest transforming potential in NIH 3T3 cells and induces both MPD and B-lymphocytic leukemia in mice, whereas the activation loop mutant C-KIT N822K only induces MPD in mice. Hence, the differences of oncogenic activities among C-KIT mutants may affect prognosis of the patients. The mouse models described here will be useful for studying the mechanisms by which C-KIT mutations contribute to myeloid leukemia development.

The concept of cooperation of AE with activating RTKs in t(8;21) AML has important clinical implications and provides a rationale to test RTK inhibitors in the treatment of patients with activating RTK mutations. Dasatinib, an ATP-competitive, dual SRC/ABL inhibitor, can inhibit BCR-ABL activation loop mutations that are found in some chronic myelogenouse leukemia patients with acquired clinical resistance to imatinib (29). Here, we tested the ability of dasatinib to inhibit the kinase activity of C-KIT mutants. Our results showed that dasatinib could be a potent inhibitor for both activation loop and juxtamembrane domain mutants of C-KIT, thus opening therapeutic perspectives for dasatinib in the treatment of leukemias with activated C-KIT abnormalities. In particular, the in vivo efficacy of dasatinib on t(8;21) leukemia was clearly demonstrated in murine AML models coexpressing AE and C-KIT N822K. Dasatinib alone prolonged survival of the diseased mice, and the compound exerted synergic effects with Ara-C in further prolonging survival of these animals.

It has been shown that imatinib only binds tyrosine kinases with an inactive conformation, whereas dasatinib can bind tyrosine kinases in their active conformation. Activation loop mutations in C-KIT were believed to activate the kinase and stabilize its active conformation (26–28). Indeed, the C-KIT activation loop mutant C-KIT D816V has been shown to be sensitive to dasatinib, although at a drug concentration much higher than that for an effective inhibition of C-KIT N822K, a distinct mutation also residing in the activation loop. However, C-KIT D816V is resistant to imatinib. On the other hand, imatinib still exerts inhibitory effects on C-KIT N822K-carrying cells. These findings suggest that different activation loop mutations may affect the C-KIT structure/function differently and that imatinib may be effective not only in patients with C-KIT juxtamembrane domain mutants but also in those with certain activation loop mutations of C-KIT. Therefore, in future designing of the clinical trial in t(8;21) AML with C-KIT activation, a reasonable use of distinct RTK inhibitors in a comparative way is warranted.

Materials and Methods

Construction of Retroviral Expression Vectors. The cDNAs containing the whole coding sequence of WT human *C-KIT*, mutated human *C-KIT N822K*, and *571+14* were cloned by RT-PCR from patients' BM samples. The RT-PCR products of *C-KIT* were digested by BamHI and XhoI and were then cloned into the BglII and XhoI multiple cloning site of retroviral vector MSCV-IRES-GFP (MigR1) upstream of the enhanced GFP gene and the IRES. To generate murine–human hybrid *C-KIT* cDNA, the extracellular region and transmembrane region of murine *c-Kit* cDNA were fused in-frame with the intracellular region of human *C-KIT* cDNA containing *N822K*, *571+14*, or *557-558Del* mutation. The resulting constructs were named *HyC-KIT N822K*, *HyC-KIT 571+14*, and *HyC-KIT 557-558Del*, respectively. *HyC-KIT WT* and *HyC-KIT D816V* were generously provided by Michael H. Tomasson (Washington University School of Medicine, Siteman Cancer Center, St. Louis, MO). The *YFP* gene was inserted by standard cloning procedure to yield the MSCV-IRES-YFP vector. The full-length *AE* cDNA was cloned by RT-PCR from kasumi-1 cell line and then subcloned into the retroviral vector to yield the MSCV-AE-IRES-YFP construct.

Retroviral Preparations and Analysis of Protein Expression. Retrovirus was produced with the constructs above by individually cotransfecting them with Pcl-Eco retrovirus packaging vector into BOSC23 cells by the calcium phosphate precipitation method as previously described (33). Retroviral supernatant was harvested 48 h after transfection, and the titer of the infectious virus was determined by flow cytometry using NIH 3T3 cells infected with serial dilutions of virus in the presence of 8 μg/mL of Polybrene. Total cell lysates from infected NIH 3T3 cells were processed for Western blot as previously described. The following primary antibodies (all 1:1,000) were used: anti-actin (AC40; Sigma-Aldrich), anti-AML1, and anti-C-KIT (Cell Signaling Technologies). HRP-labeled goat anti-mouse IgG or goat anti-rabbit IgG (Pierce Biotechnology) was used as a secondary antibody.

Cell Culture. BOSC23 cells were grown in DMEM, 10% FBS, and 1× penicillin/streptomycin. NIH 3T3 were cultured in DMEM, 10% donor bovine serum (DBS), and 1× penicillin/streptomycin. 32D, a murine IL-3–dependent myeloid cell line, was maintained in DMEM supplemented with 10% FBS, 1× penicillin/streptomycin, and 10% WEHI-3B conditional medium that contains IL-3. Primary murine BM cells were plated in transplant medium consisting of DMEM, 15% FBS, 1× L-glutamine, 56 ng/mL stem cell factor, 7 ng/mL IL-3, 12 ng/mL IL-6, 1× penicillin/streptomycin/amphotericin, and 5% WEHI-3B conditional medium.

Cell Growth and Proliferation Assays. 32D cells transduced with retrovirus were washed with DMEM thrice to remove growth factor (IL-3) and resuspended with DMEM containing 10% FBS and 1× penicillin/streptomycin 48 h after infection. Cells were plated into 12-well plates in the absence of IL-3. GFP-positive cells were determined by FACS. Transduced 32D cells were washed three times to remove IL-3 and restimulated with various concentrations of rmSCF (c-Kit ligand). Viable cells were counted daily by staining with trypan blue or evaluated by thiazolyl blue tetrazolium bromide (MTT)

assay. 32D cell lines stably expressing the control GFP were created by retroviral transduction and were sorted by GFP expression.

Soft-Agar Colony-Forming Assay. A total of 1 mL of 0.6% bottom agar [mixing 1.2% agar with concentrated media (2× DMEM plus 20% DBS plus 2× penicillin/streptomycin) with 1:1 ratio] was prepared and introduced to each well of a six-well tissue culture plate. FACS-purified NIH 3T3 cell lines expressing GFP, HyC-KIT WT, HyC-KIT D816V, HyC-KIT N822K, HyC-KIT 571+14, or HyC-KIT 557-558Del were diluted to 10^5 cells/mL, 10^4 cells/mL, or 10^3 cells/mL in 1× DMEM plus 10% DBS plus 1× penicillin/streptomycin. Triplicate 3-mL cells suspended in soft agar were added to the bottom agar for each cell line and incubated in a humidified incubator at 37 °C, 5% CO_2. Colonies were counted under a light microscope at day 10–14 after plating.

Assessment of Effects of Dasatinib on 32D Cells Expressing Mutant C-KIT. Cells were added to 24-well plates at densities of 10^5 cells per well. Dasatinib was dissolved in DMSO to create 10 mmol/L stock solutions and stored at −20 °C. Varying concentrations of dasatinib or imatinib were added, and viable cells were counted by staining with trypan blue or evaluated by MTT assay at 48 h. Dose-effect plots were created to calculate the IC_{50} for the treatment effect of dasatinib for each cell line.

BM Transduction/Transplantation. Retroviral supernatants were generated, and BM transplantation was performed as previously described (34). Briefly, BM cells were isolated from the 6- to 8-wk-old donor mice pretreated with 5-fluorouracil (250 mg/kg). BM cells were infected with retroviruses each day for 2 d in transplant medium before 5×10^5 cells were injected into the tail vein of each lethally irradiated (2×4.5 Gy, 3 to 4 h between each dose) female recipient BALB/c mouse. Retroviral titers were matched to 60% GFP^+ NIH 3T3 cells before BM infection. Recipient mice were monitored weekly for signs of disease beginning on day 14 after transplantation for 200 d and died or were killed at a terminal disease stage. Mice used in this project were purchased from Taconic Farms and were maintained in an accredited animal facility according to proper institutional guidelines.

Hematopathologic Analysis and Flow Cytometry. Smears and cytospin were stained with the Hema 3 stain set (Fisher) for routine cell morphology. Peripheral blood or single-cell suspensions of murine tissues were prepared and stained with phycoerythrin- or allophycocyanin-conjugated mouse antibodies (BD Pharmingen) for flow cytometry as previously described (35). The survival data were presented in a Kaplan-Meier format showing the percentage of mouse survival at various time points after transplantation.

Transplantation and in Vivo Treatment Studies. Primary leukemia was transplanted into 6- to 8-wk-old sublethally irradiated secondary recipient mice (4.5 Gy, 24 h before transplantation) by tail-vein injection of 1.5×10^6 leukemic cells (splenic cells) harboring both AE and HyC-KIT N822K. When the mice became moribund, they were killed, and splenic cells were isolated and inoculated into sublethally irradiated tertiary recipients (1.0×10^6 leukemic cells per mouse) for treatment. Mice were treated with vehicle (0.9% benzyl alcohol i.p. and 0.4% carboxymethyl cellulose p.o.; control group), Ara-C (25 mg/kg per day for 5 d), dasatinib, or dasatinib plus Ara-C, beginning at day 3 after leukemic cell transplantation and continuing until the death of control leukemic mice. Ara-C was dissolved in 0.9% benzyl alcohol and administered i.p. in mice. Dasatinib was suspended in 0.4% carboxymethyl cellulose and given in a dose of 10 mg/kg by oral gavage twice per day.

ACKNOWLEDGMENTS. We thank all members of the Shanghai Institute of Hematology and the R.R. laboratory for their support, and Michael H. Tomasson for providing valuable reagents. This work was supported by National Natural Science Foundation of China for Young Scholars Grant 30600362 and Shanghai Municipal Commission for Rising-Star Program Grant 08QA1404800; and in part by National High Tech Program for Biotechnology Grant 863:2006AA02A405, Chinese National Key Basic Research Project Grant 973, 2010CB529203, National Natural Science Foundation of China Grant 30821063, Key Discipline Program of Shanghai Municipal Education Commission Grant Y0201, and by the Samuel Waxman Cancer Research Foundation CoPI Program.

1. Rowley JD (2000) Molecular genetics in acute leukemia. *Leukemia* 14:513–517.
2. Peterson LF, Zhang DE (2004) The 8;21 translocation in leukemogenesis. *Oncogene* 23: 4255–4262.
3. Yergeau DA, et al. (1997) Embryonic lethality and impairment of haematopoiesis in mice heterozygous for an AML1-ETO fusion gene. *Nat Genet* 15:303–306.
4. Higuchi M, et al. (2002) Expression of a conditional AML1-ETO oncogene bypasses embryonic lethality and establishes a murine model of human t(8;21) acute myeloid leukemia. *Cancer Cell* 1:63–74.
5. Rhoades KL, et al. (2000) Analysis of the role of AML1-ETO in leukemogenesis, using an inducible transgenic mouse model. *Blood* 96:2108–2115.
6. Yuan Y, et al. (2001) AML1-ETO expression is directly involved in the development of acute myeloid leukemia in the presence of additional mutations. *Proc Natl Acad Sci USA* 98:10398–10403.
7. de Guzman CG, et al. (2002) Hematopoietic stem cell expansion and distinct myeloid developmental abnormalities in a murine model of the AML1-ETO translocation. *Mol Cell Biol* 22:5506–5517.
8. Schessl C, et al. (2005) The AML1-ETO fusion gene and the FLT3 length mutation collaborate in inducing acute leukemia in mice. *J Clin Invest* 115:2159–2168.
9. Grisolano JL, O'Neal J, Cain J, Tomasson MH (2003) An activated receptor tyrosine kinase, TEL/PDGFbetaR, cooperates with AML1/ETO to induce acute myeloid leukemia in mice. *Proc Natl Acad Sci USA* 100:9506–9511.
10. Yan M, et al. (2006) A previously unidentified alternatively spliced isoform of t(8;21) transcript promotes leukemogenesis. *Nat Med* 12:945–949.
11. Look AT (1997) Oncogenic transcription factors in the human acute leukemias. *Science* 278:1059–1064.
12. Gilliland DG, Tallman MS (2002) Focus on acute leukemias. *Cancer Cell* 1:417–420.
13. Gilliland DG, Jordan CT, Felix CA (2004) The molecular basis of leukemia. *Hematology (Am Soc Hematol Educ Program)* 2004:80–97.
14. Renneville A, et al. (2008) Cooperating gene mutations in acute myeloid leukemia: A review of the literature. *Leukemia* 22:915–931.
15. Beghini A, et al. (2004) KIT activating mutations: Incidence in adult and pediatric acute myeloid leukemia, and identification of an internal tandem duplication. *Haematologica* 89:920–925.
16. Goemans BF, et al. (2005) Mutations in KIT and RAS are frequent events in pediatric core-binding factor acute myeloid leukemia. *Leukemia* 19:1536–1542.
17. Wang YY, et al. (2005) AML1-ETO and C-KIT mutation/overexpression in t(8;21) leukemia: Implication in stepwise leukemogenesis and response to Gleevec. *Proc Natl Acad Sci USA* 102:1104–1109.
18. Jiao B, et al. (2009) AML1-ETO9a is correlated with C-KIT overexpression/mutations and indicates poor disease outcome in t(8;21) acute myeloid leukemia-M2. *Leukemia* 23:1598–1604.
19. Zheng X, Oancea C, Henschler R, Ruthardt M (2009) Cooperation between constitutively activated c-Kit signaling and leukemogenic transcription factors in the determination of the leukemic phenotype in murine hematopoietic stem cells. *Int J Oncol* 34:1521–1531.
20. Lev S, Blechman J, Nishikawa S, Givol D, Yarden Y (1993) Interspecies molecular chimeras of kit help define the binding site of the stem cell factor. *Mol Cell Biol* 13:2224–2234.
21. Xiang Z, Kreisel F, Cain J, Colson A, Tomasson MH (2007) Neoplasia driven by mutant c-KIT is mediated by intracellular, not plasma membrane, receptor signaling. *Mol Cell Biol* 27:267–282.
22. Longley BJ, et al. (1996) Somatic c-KIT activating mutation in urticaria pigmentosa and aggressive mastocytosis: Establishment of clonality in a human mast cell neoplasm. *Nat Genet* 12:312–314.
23. Hirota S, et al. (1998) Gain-of-function mutations of c-kit in human gastrointestinal stromal tumors. *Science* 279:577–580.
24. Kontogianni-Katsarou K, et al. (2008) KIT exon 11 codon 557/558 deletion/insertion mutations define a subset of gastrointestinal stromal tumors with malignant potential. *World J Gastroenterol* 14:1891–1897.
25. Ma Y, et al. (2002) The c-KIT mutation causing human mastocytosis is resistant to STI571 and other KIT kinase inhibitors; kinases with enzymatic site mutations show different inhibitor sensitivity profiles than wild-type kinases and those with regulatory-type mutations. *Blood* 99:1741–1744.
26. Foster R, Griffith R, Ferrao P, Ashman L (2004) Molecular basis of the constitutive activity and STI571 resistance of Asp816Val mutant KIT receptor tyrosine kinase. *J Mol Graph Model* 23:139–152.
27. Mol CD, et al. (2004) Structural basis for the autoinhibition and STI-571 inhibition of c-Kit tyrosine kinase. *J Biol Chem* 279:31655–31663.
28. Schindler T, et al. (2000) Structural mechanism for STI-571 inhibition of abelson tyrosine kinase. *Science* 289:1938–1942.
29. Shah NP, et al. (2004) Overriding imatinib resistance with a novel ABL kinase inhibitor. *Science* 305:399–401.
30. Schittenhelm MM, et al. (2006) Dasatinib (BMS-354825), a dual SRC/ABL kinase inhibitor, inhibits the kinase activity of wild-type, juxtamembrane, and activation loop mutant KIT isoforms associated with human malignancies. *Cancer Res* 66:473–481.
31. Boissel N, et al.; Acute Leukemia French Association (ALFA); Leucémies Aiguës Myéloblastiques de l'Enfant (LAME) Cooperative Groups (2006) Incidence and prognostic impact of c-Kit, FLT3, and Ras gene mutations in core binding factor acute myeloid leukemia (CBF-AML). *Leukemia* 20:965–970.
32. Cairoli R, et al. (2006) Prognostic impact of c-KIT mutations in core binding factor leukemias: an Italian retrospective study. *Blood* 107:3463–3468.
33. Gross AW, Zhang X, Ren R (1999) Bcr-Abl with an SH3 deletion retains the ability To induce a myeloproliferative disease in mice, yet c-Abl activated by an SH3 deletion induces only lymphoid malignancy. *Mol Cell Biol* 19:6918–6928.
34. Zhang X, Ren R (1998) Bcr-Abl efficiently induces a myeloproliferative disease and production of excess interleukin-3 and granulocyte-macrophage colony-stimulating factor in mice: a novel model for chronic myelogenous leukemia. *Blood* 92:3829–3840.
35. Parikh C, Subrahmanyam R, Ren R (2006) Oncogenic NRAS rapidly and efficiently induces CMML- and AML-like diseases in mice. *Blood* 108:2349–2357.